Published in final edited form as:

Free Radic Res. 2013 September ; 47(9): 672–682. doi:10.3109/10715762.2013.814126.

Cytotoxicity of 1,4-diamino-2-butanone, a putrescine analogue, to RKO cells: mechanism and redox imbalance

C. O. Soares[1], **M. Boiani**[2], **L. J. Marnett**[2], and **E. J. H. Bechara**[1,3]

[1]Departamento de Bioquímica, Instituto de Química, Universidade de São Paulo, São Paulo, SP, Brazil,

[2]A.B. Hancock Jr. Memorial Laboratory for Cancer Research, Vanderbilt University, Nashville, TN, USA,

[3]Departamento de Ciências Exatas e da Terra, Instituto de Ciências Ambientais, Químicas e Farmacêuticas, Universidade Federal de São Paulo, Diadema, SP, Brazil

Abstract

α-Aminocarbonyl metabolites (e.g., 5-aminolevulinic acid and aminoacetone) and the wide spectrum microbicide 1,4-diamino-2-butanone (DAB) have been shown to exhibit pro-oxidant properties. *In vitro*, these compounds undergo phosphate-catalyzed enolization at physiological pH and subsequent superoxide radical-propagated aerobic oxidation, yielding a reactive α oxoaldehyde and H_2O_2 DAB cytotoxicity to pathogenic microorganisms has been attributed to the inhibition of polyamine biosynthesis. However, the role played in cell death by reactive DAB oxidation products is still poorly understood. This work aims to clarify the mechanism of DAB-promoted pro-oxidant action on mammalian cells. DAB (0.05 – 10 mM) treatment of RKO cells derived from human colon carcinoma led to a decrease in cell viability (IC_{50} ca. 0.3 mM DAB, 24 h incubation). Pre-addition of either catalase (5 μM) or aminoguanidine (20 mM) was observed to partially inhibit the toxic effects of DAB to the cells, while *N*-acetyl-L-cysteine (NAC, 5 mM) or reduced glutathione (GSH, 5 mM) provided almost complete protection against DAB. Changes in redox balance and stress response pathways were indicated by the increased expression of HO-1, NQO1 and xCT. Moreover, the observation of caspase 3 and PARP cleavage products is consistent with DAB-triggered apoptosis in RKO cells, which was corroborated by the partial protection afforded by the pan-caspase inhibitor z-VAD-FMK. Finally, DAB treatment disrupted the cell cycle in response to increased p53 and activation of ATM. Altogether, these data support the hypothesis that DAB exerts cytotoxicity via a mechanism involving not only polyamine biosynthesis but also by DAB oxidation products.

Correspondence: Etelvino J. H. Bechara, Departamento de Ciências Exatas e da Terra, Instituto de Ciências Ambientais, Químicas e Farmacêuticas, Universidade Federal de São Paulo, DCET, Rua Prof. Artur Riedel, 275, Jardim Eldorado, Diadema, 09972-270 SP, Brazil. Tel: + 55-11-33193300. Fax: + 55-11-4043-6428. ejhbechara@gmail.com.

Declaration of interest

The authors report no declarations of interest. The authors alone are responsible for the content and writing of the paper.

Keywords

1,4-diamino-2-butanone; redox imbalance; RKO cells; apoptosis; hydrogen peroxide; α-oxoaldehyde

Introduction

The putrescine analogue 1,4-diamino-2-butanone (DAB) is a potent microbicide of a variety of parasites, including *Trypanosoma cruzi* [1,2]. DAB toxicity to these cells is reportedly attributable to the competitive inhibition of ornithine decarboxylase (ODC) [3,4], the key enzyme in the polyamine biosynthesis pathway [5]. Additionally, in *T. cruzi*, DAB has been reported to limit putrescine uptake [1]. Polyamines are essential for many cellular processes, including growth, development and differentiation [6–8]. The metabolism of polyamines has long been considered a promising target to design chemotherapeutic approaches for both cancer and various parasitoses [9]. ODC serves as an important gatekeeper in the polyamine pathway by converting L-ornithine to the diamine putrescine. In mammalian cells, ODC is short-lived (10 – 20 min) and tightly regulated at several steps from transcription to posttranslational modifications [10,11].

Previously, DAB was reported to induce oxidative stress in *T. cruzi* epimastigotes and *Leishmania amazonensis* promastigotes, as evidenced by the increase in lipid peroxidation products, loss of mitochondrial functions and cell architecture disorganization [1,12]. Medium supplementation with putrescine has been speculated to reverse the effects of DAB because, in addition to contributing to the expression of genes related to the cell defense response [13,14], putrescine exhibits antioxidant properties [15]. Maia et al. [4] reported that the addition of aminoguanidine, a polyamine/diamine oxidase inhibitor and Schiff condensation agent of α-oxoaldehydes [16], partially reversed the effects of DAB, which is in agreement with the hypothesis that DAB oxidation products, H_2O_2 and 4-amino-2-oxobutanal (oxoDAB), play a significant role in DAB-induced cell death [17]. Indeed, similar to other α-aminoketones [18] such as aminoacetone [19] and 5-aminolevulinic acid [20], DAB has previously been shown to undergo metal-catalyzed oxidation in phosphate buffer, yielding reactive oxygen species (ROS), NH_4^+ ion, and 4-amino-2-oxobutanal (oxoDAB), a potentially toxic α-oxoaldehyde [17].

To explore the potential of DAB to induce cell death via production of ROS and DNA damage, we investigated DAB effects on mammalian cells. We employed the human colon carcinoma cell line, RKO, which has been extensively used to investigate molecular mechanisms of cell damage in response to oxidants and electrophiles [21,22]. The results of our investigations support the hypothesis that DAB can induce cell death by mechanisms associated with thiol-linked redox imbalance and DNA damage.

Materials and methods

Cell culture and treatment

RKO cells, a p53 wild-type human colon carcinoma cell line, were maintained in DMEM (Invitrogen, Carlsbad, CA) supplemented with 10% fetal bovine serum (FBS, Atlas, Fort

Collins, CO) at 37°C and 5% CO_2. A 100 mM stock solution of DAB (Sigma, St. Louis, MO) was freshly prepared in MilliQ®-purified water. Stock solutions of catalase aminoguanidine, buthionine sulfoximine (BSO), *N*-acetyl-L-cysteine (NAC), and reduced glutathione (Sigma, St. Louis, MO) were prepared in PBS (Invitrogen, Carlsbad, CA).

Viability assay

RKO cells were seeded in 96-well plates at a density of 8,000 cells/well 24 h prior to treatments. All cell treatments were carried out in phenol red-free OptiMEM-reduced serum medium. After an established time-point incubation, the cell medium was replaced by DMEM supplemented with 10% FBS. After 48 h, cell viability was determined using WST-1 (Roche, Indianapolis, IN), a cellimpermeable reagent that yields a water soluble formazan product via NAD(P)H-dependent cellular oxidoreductases, according to the manufacturer's protocol.

Detection of intra and extracellular redox status

Intracellular redox status was assayed by the oxidation of 2',7'-dichlorofluorescein diacetate (DCFH-DA) [23,24]. RKO cells were seeded in 96-well plates at a density of 12,000 cells/well. After 24 h, the cells were pre-loaded with freshly prepared 30 μM DCFH-DA in phenol red-free OptiMEM-reduced serum medium for 60 min at 37°C. Next, the cells were rinsed thrice with PBS at room temperature and treated with either DAB or H_2O_2 in OptiMEM. Oxidized DCF fluorescence was measured using an Infinite 200 PRO Multiwell plate reader (Tecan, Mannedorf, Switzerland) with excitation and emission wavelengths of 488 and 530 nm, respectively.

Extracellular ROS was accessed by nitroblue tetrazolium (NBT) formazan product in cell medium. LLC-MK2 cells were incubated with DAB in presence of 0.1% NBT prepared in phenol red free-MEM for 3 h at 37°C. Control assays were performed in the absence of the cell culture. The formazan product in the medium was measured using Synergy HT microplate reader (Biotek, Winooski, VT) at 560 nm.

Assay of total reduced thiols and GSH

Total free thiols were measured by a reaction with monobromobimane (mBBr) leading to the formation of a stable fluorescent adduct [25,26]. RKO cells were seeded in a 6-well plate at a density of 3.5×10^5 cells/well. After 24 h, the cells were treated with either DAB or H_2O_2 for 5 h in OptiMEM. The cells were then incubated in the dark at room temperature for 10 min in 0.8 mM mBBr in PBS. Cell pellets were obtained by centrifugation at 5,000 g for 5 min, rinsed twice with PBS and lysed with M-Per buffer (Thermo, Waltham, MA). Protein precipitation was conducted with TCA (10%, final concentration), followed by centrifugation at 14,000 g for 10 min. The supernatant was used to measure low molecular weight thiols, and the protein pellet was resuspended in 10 mM Tris-HCl (pH 7.4) containing 1% SDS. The fluorescence of bimane-adducts was measured using a SpectraMax Multiwell plate reader (Molecular Devices, Sunnyvale, CA) with excitation and emission wavelengths of 394 and 480 nm, respectively.

GSH levels were accessed by the reaction with DTNB (5,5′-dithio-bis(2-nitrobenzoic acid)) according to the enzymatic recycling method described by Rahman et al. [27]. RKO cells were seeded in a 6-well plate at a density of 3.5×10^5 cells/well. After 24 h, the cells were pretreated with 100 μM BSO or 5 mM NAC in phenol free-MEM, supplemented with 2% FBS. Subsequently (24 h) the cells were treated with DAB for 5 h. The cell pellet was lysed in 0.10 M phosphate buffer containing 5 mM EDTA, 0,06% sulfosalicylic acid and 0.1% Triton X-100, After 30 min in ice the samples were centrifuged at 14,000 g for 10 min at 4°C. The supernatant was incubated with 2-vinylpyridine for 1 h at RT and, after addition of triethanolamine, GSH was quantified by treating the samples with DTNB in the presence of glutathione reductase and NADPH, using a standard curve of GSH normalized by protein levels.

Western blotting

Cell pellets were lysed on ice using M-Per lysis buffer (Thermo, Waltham, MA) containing protease and phosphatase inhibitor cocktail (Sigma, St. Louis, MO). Debris from cell lysate was cleared by centrifugation at 14,000 g for 10 min. The supernatant was then recovered, and protein concentrations were quantified by the bicinchoninic acid protein assay (Thermo, Waltham, MA) using bovine serum albumin as a standard. Proteins (15 μg) were resolved by SDS-PAGE (4 – 20%) under reducing conditions and transferred to 0.2 μM nitrocellulose membranes (Bio-Rad, Hercules, CA). The mem-branes were blocked for 1 h at RT in TTBS (20 mM Tris, pH 7.5, 140 mM NaCl, and 0.05% Tween 20, containing 5% nonfat dry milk) and incubated with primary and secondary antibodies. The following primary antibodies were used: caspase 3, PARP, p53, phospho-JNK, JNK, cyclin B1, and phospho-ATM (Cell Signaling, Danvers, MA); α-actin and ATM (Santa Cruz Biotechnology, St. Cruz, CA); and HO-1 and cyclin F (BD Biosciences, San Diego, CA). The following secondary antibodies were employed: anti-mouse and anti-rabbit HRP conjugate (Promega, Madison, WI) and anti-goat HRP conjugate (Santa Cruz Biotechnology, St. Cruz, CA).

RNA extraction and real-time PCR

Total RNA was collected using the RNeasy collection kit (Qiagen, Germantown, MD). One microgram of total RNA was used in each reverse transcription reaction with the iScript reagent (Bio-Rad, Hercules, CA). One-tenth of each reaction volume (2 μl) was used per replicate in the subsequent real-time PCR (RT-PCR) analysis using the iQ SYBR Green Supermix (Bio-Rad, Hercules, CA). Real-time reactions were performed using a Bio-Rad iCycler real time machine. The following primer sequences were used: HMOX-1, upper 5’-GGGGGCCAGGTGCTCAAAAAGATT-3’, lower 5’-GAGTTCATGCGGGAGCGGTAGAGC-3’; xCT, upper 5’-GTCCGCAAGCACACTCCTCTAC-3’, lower 5’-AG CAACTGCCAGCCCAATAAA-3’; NQO1, upper 5’-GTAAACTGAAGGACCCTGCGAACT-3’, lower 5’-GGGGAACTGGAATATCACAAGGTC-3’; Nrf-2, upper 5’-TCAGCCAGCCCAGCACATCCAGTC-3’, lower 5’ AGCCGAAAGAAACCTCATTGTCATC-3’; and GAPDH, upper 5’-GCCTCAAGATCATCAGCAAGT-3’, lower 5’-CTTCCACGATACCAAAGTTGTC-3’.

Flow cytometry assays

Cell cycle analysis was carried out at a density of 2×10^6 cells/ml fixed in cold 70% ethanol in PBS overnight at 4°C. Cells were then washed with PBS and stained with 50 μg/mL of a propidium iodide solution (Sigma, St. Louis, MO) in PBS containing 50 μg/mL of RNase A (Qiagen, Germantown, MD) for 30 min. The samples were analyzed by a 5 Laser LSRII flow cytometer (BD Biosciences, San Diego, CA) in the VMC Flow Cytometry Shared Resource, according to Furuya et al. [28] and Darzynkiewicz et al. [29].

Statistical analysis

The data represent at least three independent experiments and are expressed as the means ± SD. Student's t test or ANOVA was employed for statistical analysis with a significance of at least $p < 0.05$.

Results

DAB decreases RKO viability by inducing oxidative stress

Figure 1 demonstrates the viability of RKO cells in the presence of 0 – 2.0 mM DAB, revealing that DAB exerts significant toxicity only above 0.50 mM, which is three times more toxic over 24 h incubation compared to a 5 h incubation (Figure 1A). However, there was no dose response above 1.0 mM DAB. This could tentatively be explained by condensation of oxoDAB with remaining DAB, ultimately yielding a pyrrolidone adduct [16]. DAB toxicity plateaued at 24 h, the IC_{50} value being estimated to be *ca.* 0.3 mM (Figure 1B).

DAB was indicated to induce intracellular changes in redox status by the dose-and time-dependent fluorescence increase (50 – 80%) of 0.10 – 0.30 mM DCFDA exposed to the cells for 30 and 60 min (Figure 2A). As expected, a positive control experiment carried out with 0.2 mM H_2O_2 displayed higher indices of DCFDA fluorescence due to the limitation of intracellular H_2O_2 generation by DAB oxidation. In contrast, DAB clearly modified the extracellular redox status, as indicated by increased reduction of NBT dependent on DAB concentration (Figure 2B). Cell-free experiments conducted with NBT in phenol free-MEM containing different concentrations of DAB suggested that DAB oxidation takes place mainly outside the cells. Control experiments conducted with 0.3 mM DAB in the presence of 50 U CuZnSOD confirm $O_2^{\bullet -}$ production by DAB oxidation in the culture medium as well. Thus, the observed lower amount of NBT reduction in presence of the cells may reflect changes in the intracellular redox status. On the basis of the concentration of the cyclic end product of DAB oxidation in the medium as a parameter for DAB cell uptake, we found no differences in presence or absence of the cells at the same concentrations of DAB (not shown). Altogether these data suggest that DAB undergoes oxidation mainly outside the cells and that extracellular DAB-generated H_2O_2 diffuses across the cell membrane causing cell damage and death.

The levels of thiols in both protein and soluble fractions of lysed cells (Figure 3A) were also analyzed. Cell incubations with 0.30 – 0.50 mM DAB for 5 h significantly decreased the levels of total thiols, mainly glutathione (GSH), present in the soluble fraction (15 – 20%). A

positive control containing 0.50 mM H_2O_2 resulted in 45% less thiols. No differences in precipitated protein thiols were detected upon cell treatment with either DAB or H_2O_2. In order to verify the role of GSH on DAB toxicity, the cells were pretreated with 100 μM BSO, an inhibitor of GSH synthesis, or 5 mM NAC, as a positive control of the experiment, and subsequently with 0.3 mM DAB for 24 h. The viability assays (Figure 3B) indicate that pretreatment with BSO increases 1.6-fold the DAB toxicity to RKO cells. Conversely, NAC affords robust cell protection against DAB, despite the unanticipated NAC toxicity observed in control cells. GSH and total thiols assays also corroborate these findings (Figure 3C). DAB treatment leads to a 25% decrease of GSH in the cell compartments, while parallel pretreatment with BSO/DAB reduced GSH levels by 40%, which correlates to increased DAB cytotoxicity. As expected, pretreatment with NAC not only maintained the levels of GSH but also showed to induce GSH biosynthesis, which may be associated to protection against DAB.

In an attempt to demonstrate that DAB toxicity to RKO cells is mediated by H_2O_2 and/or oxoDAB produced by DAB oxidation, we supplemented the culture medium with either catalase (5 μM), a H_2O_2 scavenger, or aminoguanidine (20 mM), a nucleophilic agent toward oxoDAB and other α-oxoaldehydes (Figure 4) [16]. Previous work showed that GSH or catalase addition decreased the observed rate of Cu(II)-catalyzed DAB oxygen uptake by 50 and 83%, respectively [17]. Here, the addition of extracellular catalase only partially (15% at 0.3 mM DAB) protected the cells against DAB-produced H_2O_2 (Figure 4). Similar result was obtained upon addition of aminoguanidine to the cell medium. Conversely, medium supplementation with either NAC (5 mM) or GSH (5 mM) afforded strong protection against DAB toxicity, probably due to fast nucleophilic addition of the GSH cysteine residue to the oxoDAB in addition to GSH oxidation by H_2O_2, among other protective biological systems. DAB cytotoxicity to mammalian RKO cells operates in part by triggering an oxidative stress mechanism, as previously demonstrated by Soares et al. [2,17] when incubating DAB with a kidney-derived epithelial cell line. Accordingly, Maia et al. [4] reported the pro-oxidant effects of DAB on *T. cruzi* with aminoguanidine, which prevented lipoperoxidation and mitochondrial damage induced by DAB.

Aiming to verify the effect of DAB end products on cell viability an aged solution of 10 mM DAB in PBS at 37°C for 24 h (Figure 5A), putatively rich in oxoDAB and its condensation products, was used. The extent of cell viability decline was similar to that observed with freshly added 1.0 mM DAB. This finding does not exclude the possibility that remaining, not-reacted DAB induces the decay of cell viability. Conversely, DAB freshly added to the cell culture is expected to form ROS and oxoDAB during the 24 h incubation time. No effect on cell viability was observed when the DAB solution was aged in presence of 20 mM of either NAC or GSH, which are known to react with ROS and α-oxoaldehydes [30,31], The absorption spectra of aged DAB in presence of NAC or GSH confirm the occurrence of such reactions (Figure 5B). On the other hand, DAB solution previously aged in presence of 20 mM aminoguanidine leads to a product with absorption spectrum similar to that exhibited by DAB end products (Figure 5B) and triggers similar toxicity to RKO cells (Figure 5A).

DAB induces the expression of antioxidant proteins in RKO cells

Initially, the expression of HO-1 (heme oxygenase 1), a key antioxidant enzyme inducible under oxidative stress that is controlled by the transcription factor Nrf-2 [32] was examined (Figure 6A, B). The cyto-protective effect of HO-1 is attributed to the generation of CO and bilirubin during the heme degradation catalyzed by the enzyme. Both products are putatively related to antioxidant defense in cells [33,34]. RKO cell treatment with 0.30 mM DAB over 24 h was found to significantly induce HO-1 expression, which was verified by the increase in both protein (Figure 6A) and mRNA (Figure 6B) levels.

In addition, changes in the expression of the transcription factor Nrf-2 and related genes upon DAB treatment were studied (Figure 6C). Nrf-2 is known to regulate a battery of genes in response to oxidative and/or electrophilic stress [35]. DAB-generated H_2O_2 and oxoDAB represent an oxidizing and a Schiff-adducting stimulus to cells, respectively. Accordingly, DAB treatment of RKO cells augmented the Nrf-2-controlled expression of the HO-1, NQO-1 (NAD(P)H quinone acceptor oxidoreductase 1) and xCT (cysteine/glutamate exchange transporter) genes in a dose-dependent manner.

DAB treatment activates apoptosis and affects the cell cycle

Once DAB was confirmed to decrease cell viability, chemical changes in redox metabolites and the induction of enzymatic antioxidant responses, the ability of DAB to activate apoptosis was investigated. Cleaved products of caspase 3 and PARP (poly(ADP-ribose) polymerase), extensively employed to characterize the apoptotic route, were consistently observed after 24 h of treatment of RKO cells with 0.30 mM DAB (Figure 7A).

In addition, the levels of SAPK/JNK (stress-activated protein kinase/c-Jun N-terminal protein kinase), putative apoptosis mediators under distinct stimulus and cellular conditions [36], were observed to respond positively to DAB administration. Interestingly, only the 46 kDa SAPK/JNK isoform was phosphorylated, suggesting that the effect of DAB on cells is an early event (Figure 7A).

To verify the DAB effect on caspase activation, cells were treated with the pan-caspase inhibitor z-VAD-FMK (10μM) prior to DAB treatment (0.3 mM). A decrease in cell viability was observed, which was attenuated by approximately 15% (Figure 7B), suggesting that the drop in cell viability caused by DAB is not completely related to caspase cascade activation. No significant effect was observed using higher concentrations of z-VAD-FMK (data not shown).

The effect of DAB on RKO cell cycle progression was evaluated by staining DAB-treated cells (0.30 mM, 24 h incubation) with propidium iodide and submitting them to FACS analysis. Interestingly, the cell population in the G1 phase was strongly reduced by approximately 26% (Figure 8A), and the population in the G2 phase increased by 10%, thereby indicating that DAB compromises the RKO cell cycle. A dramatic increase of the sub G0 cell population (≈ 15%) under DAB treatment was also observed, which is consistent with DAB-triggered RKO cell apoptosis. Disruption of the cell cycle is related to DNA damage. Therefore, we checked the levels and activation of certain proteins related to DNA repair and cell cycle control (Figure 8B). The protein kinase ataxia telangiectasia

mutated (ATM) is one of the early signaling events activated in response to DNA damage [37]. DAB treatment led to phosphorylation of ATM, the active form of this protein, as shown in Figure 8B. Downstream of the ATM pathway are checkpoint kinases 1 and 2 (Chk1 and Chk2). No significant effect was observed in the levels of these proteins after DAB treatment (not shown). In addition, cyclin B1 and F, which are proteins responsible for the progression of the G2/M cell cycle phase, were not affected by DAB treatment. On the other hand, the expression of the tumor suppressor p53, which increases mainly in response to DNA damage [38], was stimulated upon DAB treatment (Figure 8B). However, neither phospho-p53 nor p53 mRNA alterations were observed during the same DAB treatments (data not shown).

Discussion

DAB is a putrescine analogue, which was previously described as a competitive inhibitor of ODC [39]. Menezes et al. [1] recently reported the anti-proliferative activity of DAB on *T. cruzi* epimastigotas and more recently, Soares et al. [2] verified similar effect of DAB on *T. cruzi* trypomastigotes. Interestingly, *T. cruzi* lacks ODC. As a result, *T. cruzi* is unable to carry out *de novo* biosynthesis of putrescine and depends on exogenous polyamines present in the culture medium [40,41]. In this context, the proposed pro-oxidant potential of DAB [17], a promptly oxidizable α-aminoketone yielding H_2O_2 and α-oxoaldehyde (oxoDAB), to explain the microbicide toxicity seems attractive and plausible. Therefore, we employed DAB-treated RKO cell cultures to elucidate the mechanism of DAB-induced cell death by virtue of the short half-life of ODC in mammalian cells [9].

Here, we report that DAB leads to a decrease in the viability of RKO cells in a concentration-and time-dependent manner, resulting in an IC_{50} value of 0.30 mM after 24 h of incubation (Figure 1B). The observed protective effect of added catalase and aminoguanidine, albeit moderate (15%), and the strong effect of NAC and GSH (Figure 4) suggest participation of deleterious DAB oxidation products (H_2O_2 and oxoDAB) in cell viability. Similar results were obtained with RINm5f cells treated with aminoacetone, a DAB analogue, in the presence and absence of catalase [42]. On the other hand, 2-difluoromethylornithine (DFMO), a specific inhibitor of ODC, has been reported to be effective only at high concentrations (1 – 5 mM) and a long incubation time (3 – 10 days) in different tumor cell lines [43–45]. These findings reinforce the hypothesis that DAB cytotoxicity might be related to oxidative stress because lower DAB concentrations and shorter incubation times suffi ce to induce cell death compared to that of DFMO.

Despite the lower ability of DAB to oxidize intracellular DCFH as compared to H_2O_2, (Figure 2A), DAB is shown here to augment the cellular oxidized status (Figure 2B), which is suggested by the observed decreased low molecular weight thiol concentrations in RKO cells (Figure 3A). It is well documented that thiols constitute the major defense mechanism against oxidative stress [46,47]. Changes in the GSH/GSSG ratios were also observed when glioma cells were treated with aldehydes such as 3-aminopropanal [48]. Reactive aldehydes, such as α,β-unsaturated alkenals (*e.g.*, acrolein), α-oxoaldehydes (e.g., methylglyoxal, oxoDAB), and alkanals, are expected to be highly cytotoxic due to their adduction to protein amino acid residues and nucleobases [49,50]. Accordingly, GSH (Figure 3B, C) and

probably oxoDAB (Figures 4 and 5) are shown here to play important role on DAB cytotoxicity. DAB-induced redox imbalance was corroborated by the inhibitory effect that results from addition of either NAC or GSH (Figure 4).

In addition to changes in the cell redox status, DAB was shown to induce the activation of the transcription factor Nrf-2 (Figure 6B), a member of the basic leucine-zipper NF-E2 family that interacts with the antioxidant response element (ARE), leading to up-regulation of downstream genes coding for phase II detoxification enzymes and antioxidant enzymes [51]. Under stress conditions, Nrf-2 dissociates from Keap1, thereby rescuing Nrf-2 from proteosomal degradation and allowing its translocation to the nucleus [52]. Many stressors are responsible for activating Nrf-2 cell response, such as ROS, aldehydes, heavy metals, electrophilic xenobiotics and corresponding metabolites [53]. In addition, Nrf-2 regulates the expression of diverse genes that comprise the antioxidant response in the cell. Among these genes are the following: (i) HO-1, the isoenzyme that affords protection against programmed cell death, catabolizing free heme into equimolar amounts of Fe^{2+}, carbon monoxide and biliverdin [23]; (ii) NQO1, a FAD-binding protein that promotes two-electron reduction of quinones and other derivatives, thereby slowing down the redox cycling of these compounds and creating the opportunity of ROS generation [54] and (iii) xCT, a cysteine media-tor transporter that is important for maintaining intracellular GSH levels [55]. Importantly, DAB treatment of RKO led to not only increased expression of Nrf-2 but also augmented expression of HO-1 (Figure 6A), NQO1 and xCT (Figure 6B). These data support the hypothesis that DAB acts as a pro-oxidant xenobiotic, resulting in the concomitant enhancement of antioxidant defenses. Likewise, toxic metabolites of polyamine catabolism induce genes that promote cell survival, such as GST and NQO1, mediated through the Nrf-2 response [56]. Microarray analysis of the RKO cell line treated with 0.10 and 0.30 mM DAB incubated for 24 h confirmed the aforementioned findings. Changes ranging from 1.5-to 2.5-fold were measured for the transcripts HO-1, GCLM (glutamate-cysteine ligase regulatory subunit, the first rate limiting enzyme in the GSH synthesis), and NQO1 principally using 0.30 mM DAB during 24 h of incubation (data not shown).

A bulk of data has pointed out that imbalances between ROS production and antioxidant defenses lead to the disruption of cellular metabolism due to the chemical damage of proteins, lipids, polysaccharides, and DNA. The degree of cellular damage determines the type of death mechanisms that are activated [57]. Despite the cytoprotection provided by enzymatic systems in response to the pro-oxidant effects of DAB, a significant decrease in cell viability was observed (Figure 1A). DAB administration was shown to activate apoptosis in RKO cells, as evidenced not only by the induction of the caspase system (Figure 7A) and the protective effect of the pan-caspase inhibitor z-VAD FMK on cell viability (Figure 7B), but also by an increased cell population in sub G0 phase (Figure 8A). In addition, the partial activation of the c-Jun N-terminal kinase was observed in DAB-treated cells (Figure 7A). Interestingly, JNK activity can modulate apoptosis, proliferation or survival, depending on the cellular conditions, whereas a strong stress stimulus leads to JNK-mediated apoptosis [58]. Apoptosis in RINmf5 cells, an insulin-producing pancreatic cell line, has also been reported to trigger oxidative stress when cells are treated with aminoacetone, an α-aminoketone analogous to DAB [33].

Additionally, DAB was shown to change the cell cycle progression of RKO cells (Figure 8A) by partially blocking the cells in G2/M phase, as suggested by the increased levels of p53 (Figure 8B) needed to maintain G2 arrest, which involves the initial inhibition of cyclin B followed by the up-regulation of downstream-related genes [59,60]. Checkpoint controls allow cell cycle arrest, preventing the dissipation of errors in DNA and any other stress signals. Either cell cycle arrest or apoptosis, both mediated by p53 [36], can explain the cell damage. In this regard, cell exposure to aldehydes, ROS and ionizing radiation result in the introduction of double-strand breaks into cellular DNA [61]. The cell responds to DNA damage by activating ATM through the auto-phosphorylation of serine 1981. The resulting activated ATM assists in the phosphorylation of downstream substrates, such as p53 [35]. The presence of phospho-ATM in RKO cells treated with DAB strongly supports the idea of DAB acting as a pro-oxidant molecule (Figure 8B). Furthermore, 5-aminolevulinic acid, an α-aminoketone chemically similar to DAB, was previously demonstrated to induce dose-dependent damage in the nuclear DNA of human SVNF fibroblasts and CHO cells [62].

Among other factors, polyamines exert a critical role in cell cycle progression because they regulate the interaction sites between cyclins and cyclin-dependent kinases (CDKs) [5]. Additionally, the depletion of polyamines over the long-term administration of DFMO (5 mM) was found to inhibit growth and arrest the following cells in G1 phase: human breast cancer [63], retinoblastoma Y79 cells [64] and HeLa cells [65]. Conversely, the number of DAB treat-cells significantly decreased in G1 phase and consequently led to putative G2 cell arrest, indicating that DAB cytotoxicity is mediated by oxidative stress.

Figure 9 summarizes our proposal to clarify the molecular mechanisms underlying the cytotoxicity of DAB to mammalian cells involving H_2O_2, oxoDAB and the pool of thiols. In conclusion, our findings support the hypothesis that oxidative stress contributes to the mechanism of DAB cytotoxicity to mammalian cell lines and potentially to pathogenic microorganisms, such as *T. cruzi* and several fungi.

Acknowledgments

We are grateful to Dr. Maria Julia Manso Alves (IQUSP, Brazil) for helpful discussions and kindly reading this manuscript.

This work was supported by the Fundação de Amparo à Pesquisa do Estado de São Paulo (FAPESP), the Conselho Nacional de Desenvolvimento Científico e Tecnológico (CNPq), the Coordenação de Aperfeiçoamento de Pessoal de Nível Superior (CAPES), INCT Processos Redox em Biomedicina – Redoxoma, and the National Institute of Environmental Health Sciences (NIEHS grant 5P01ES013125).

References

[1]. Menezes D, Valentim C, Oliveira MF, Vannier-santos MA. Putrescine analogue cytotoxicity against *Trypanosoma cruzi*. Parasitol Res 2006; 98: 99–105. [PubMed: 16283411]

[2]. Soares CO, Colli W, Alves MJM, Bechara EJH. 1,4-Diamino-2-butanone a putrescine analogue promotes redox imbalance in *Trypanosoma cruzi* and mammalian cells. Arch Biochem Biophys 2012; 528: 103–107. [PubMed: 23036870]

[3]. Ueno Y, Fukumatsu M, Ogasawara A, Watanabe T, Mikami T, Matsumoto T. Hyphae formation of *Candida albicans* is regulated by polyamines. Biol Pharm Bull 2004; 27: 890–892. [PubMed: 15187439]

[4]. Maia C, Lanfredi-Rangel A, Santana-Anjos KG, Oliveira MF, Souza W, Vannier-Santos MA. Effects of a putrescine analog on *Giardia lamblia*. Parasitol Res 2008; 103: 363–37. [PubMed: 18437421]

[5]. Pegg AE. Polyamine metabolism and its importance in neo-plastic growth and target for chemotherapy. Cancer Res 1988; 48: 759–774. [PubMed: 3123052]

[6]. Rajeeve V, Pearce W, Cascante M, Vanhaesebroeck B, Cutillas PR. Polyamine production is downstream and upstream of oncogenic PI3K signalling and contributes to tumour cell growth. Biochem J 2013; 450: 619–628. [PubMed: 23330613]

[7]. Colotti G, Ilari A. Polyamine metabolism in Leishmania: from arginine to trypanothione. Amino Acids 2011; 40: 269–285. [PubMed: 20512387]

[8]. Igarashi K, Kashiwagi K. Modulation of cellular function by polyamines. Int J Biochem Cell Biol 2010; 42: 39–51. [PubMed: 19643201]

[9]. McCann PP, Pegg AE. Ornithine decarboxylase as an enzyme target for therapy. Pharmacol Ther 1992; 54: 195–215. [PubMed: 1438532]

[10]. Manen CA, Russell DH. Regulation of RNA polymerase I activity by ornithine decarboxylase. Biochem Pharmacol 1977; 26: 2379–2384. [PubMed: 597325]

[11]. Pegg AE. Regulation of ornithine decarboxylase. J Biol Chem 2006; 281: 14529–14532. [PubMed: 16459331]

[12]. Vannier-Santos MA, Menezes D, Oliveira MF, Mello FG. The putrescine analogue 1,4-diamino-2-butanone affects polyamine synthesis transport ultrastructure and intracellular survival in *Leishmania amazonensis*. Microbiology 2008; 154: 3104–311. [PubMed: 18832316]

[13]. Thackenkova AG, Nesterova LY. Polyamines as modulators of gene expression under oxidative stress in *Escherichia coli*. Biochemistry (Mosc) 2003; 68: 850–856. [PubMed: 12948384]

[14]. Rhee HJ, Kim EJ, Lee JK. Physiological polyamines: simple primordial stress molecules. J Cell Mol Med 2007; 11: 685–703. [PubMed: 17760833]

[15]. Tkachenko AG, Akhova AV, Shumkov MS, Nesterova LY. Polyamines reduce oxidative stress in *Escherichia coli* cells exposed to bactericidal antibiotics. Res Microbiol 2012; 163:83–91. [PubMed: 22138596]

[16]. Thornalley PJ. Use of aminoguanidine (Pimagedine) to prevent the formation of advanced glycation endproducts. Arch Biochem Biophys 2003; 419: 31–40. [PubMed: 14568006]

[17]. Soares CO, Alves MJ, Bechara EJH. 1,4-Diamino-2-butanone a wide-spectrum microbicide yields reactive species by metalcatalyzed oxidation. Free Radic Biol Med 2011; 50: 1760–1770. [PubMed: 21466850]

[18]. Bechara EJH, Dutra F, Cardoso VES, Sartori A, Olympio KPK, Penatti CAA, et al. The dual face of endogenous α-aminoketones: pro-oxidizing metabolic weapons. Comp Biochem Physiol Part C 2006; 146: 88–110.

[19]. Dutra F, Knudsen FS, Curi D, Bechara EJH. Aerobic oxidation of aminoacetone a threonine catabolite: iron catalysis and coupled iron release from ferritin. Chem Res Toxicol 2001; 14: 1323–1329. [PubMed: 11559049]

[20]. Monteiro HP, Abdalla DS, Augusto O, Bechara EJ. Free radical generation during delta-aminolevulinic acid autoxidation: induction by hemoglobin and connections with porphyrinpathies. Arch Biochem Biophys 1989; 271: 206–216. [PubMed: 2540713]

[21]. West JD, Ji C, Duncan ST, Amarnath V, Schneider C, Rizzo CJ, et al. Induction of apoptosis in colorectal carcinoma cells treated with 4-hydroxy-2-nonenal and structurally related aldehydic products of lipid peroxidation. Chem Res Toxicol 2004; 17: 453–462. [PubMed: 15089087]

[22]. Codreanu SG, Zhang B, Sobecki SM, Billheimer DD, Liebler DC. Global analysis of protein damage by the lipid electrophile 4-hydroxy-2-nonenal. Mol Cell Proteomics 2009; 8: 670–680. [PubMed: 19054759]

[23]. Oyama Y, Hayashi A, Ueha T, Maekawa K. Characterization of 2’7’-dichlorofluorescin fluorescence in dissociated mam-malian brain neurons: estimation on intracellular content of hydrogen peroxide. Brain Res 1994; 635: 113–117. [PubMed: 8173945]

[24]. Trayner ID, Rayner AP, Freeman GE, Farzaneh F. Quantitative multiwell myeloid differentiation assay using dichlorodihy-drofluorescein diacetate (H2DCF-DA) or dihydrorhodamine 123 (H2R123). J Immunol Meth 1995; 186: 275–284.

[25]. Weis M, Cotgreave IC, Moore GA, Norbeck K, Mold é us P. Accessibility of hepatocyte protein thiols to monobromobimane. Biochim Biophysis Acta 1993; 1176: 13–19.

[26]. Anderson MT, Trudell JR, Voehringer DW, Tjioe IM, Herzenberg LA, Herzenberg LA. An improved monobromobimane assay for glutathione utilizing tris-(2-carboxyethyl) phosphine as the reductant. Anal Biochem 1999; 272: 107–109. [PubMed: 10405300]

[27]. Rahman I, Kode A, Biswas SK. Assay for quantitative determination of glutathione and glutathione disulfide levels using enzymatic recycling method. Nat Protoc 2006; 1: 3159–3165. [PubMed: 17406579]

[28]. Furuya T, Kamada T, Murakami T, Kurose A, Sasaki K. Laser scanning cytometry allows detection of cell death with morphological features of apoptosis in cells stained with PI. Cytometry 1997; 29: 173–177. [PubMed: 9332824]

[29]. Darzynkiewicz Z, Bedner E, Li X, Gorczyca W, Melamed MR. Laser-scanning cytometry: a new instrumentation with many applications. Exp Cell Res 1999; 249: 1–12. [PubMed: 10328948]

[30]. Zeng J, Davies MJ. Evidence for the formation of adducts and S-(carboxymethyl)cysteine on reaction of alpha-dicarbonyl compounds with thiol groups on amino acids peptides and proteins. Chem Res Toxicol 2005; 18: 1232–1241. [PubMed: 16097796]

[31]. Baker LM, Baker PR, Golin-Bisello F, Schopfer FJ, Fink M, Woodcock SR, et al. Nitro-fatty acid reaction with glutathione and cysteine Kinetic analysis of thiol alkylation by a Michael addition reaction. J Biol Chem 2007; 282: 31085–31093. [PubMed: 17720974]

[32]. Gozzelino R, Jeney V, Soares MP. Mechanisms of cell protection by heme oxygenase-1. Annu Rev Pharmacol Toxicol 2010; 50: 323–354. [PubMed: 20055707]

[33]. Wegiel B, Chin BY, Otterbein LE. Inhale to survive cycle or die? Carbon monoxide and cellular proliferation. Cell Cycle 2008; 7: 1379–1384. [PubMed: 18418071]

[34]. Jansen T, Hortmann M, Oelze M, Optiz B, Steven S, Schell R, et al. Conversion of biliverdin to bilirubin by biliverdin reductase contributes to endothelial cell protection by heme oxygenase-1-evidence for direct and indirect antioxidant actions of bilirubin. J Mol Cell Cardiol 2010; 49: 186–195. [PubMed: 20430037]

[35]. Ma Q, He X. Molecular basis of electrophilic and oxidative defense: promises and perils of Nrf2. Pharmacol Rev 2012; 64: 1055–1081. [PubMed: 22966037]

[36]. Weston CR, Davis RJ. The JNK signal transduction pathway. Curr Opin Cell Biol 2007; 19: 142–149. [PubMed: 17303404]

[37]. Bakkenist CJ, Kastan MB. DNA damage activates ATM through intermolecular autophosphorylation and dimer dissociation. Nature 2003; 421: 499–506. [PubMed: 12556884]

[38]. Vousden KH, Lu X. Live or let die: the cell's response to p53. Nature Rev Cancer 2002; 2: 594–604. [PubMed: 12154352]

[39]. Stevens L, McKinnon IM, Winther M. The effects of 14-diaminobutanone on polyamine synthesis in *Aspergillus nidulans*. FEBS Lett 1977; 75: 180–182. [PubMed: 323046]

[40]. Ariyanayagam MR, Fairlamb AH. Diamine auxotrophy may be a universal feature of *Trypanosoma cruzi* epimastigotas. Mol Biochem Parasitol 1997; 84: 111–121. [PubMed: 9041526]

[41]. Carrillo C, Cejas S, González NS, Algranati ID. *Trypanosoma cruzi* epimastigotes lack ornithine decarboxylase but can express a foreing gene enconding this enzyme. FEBS Lett 1999; 454: 192–196. [PubMed: 10431805]

[42]. Sartori A, Garay-Malpartida HM, Forni MF, Schumacher RI, Dutra F, Sogayar MC, Bechara EJ. Aminoacetone a putative endogenous source of methylglyoxal causes oxidative stress and death to insulin-producing RINm5f cells. Chem Res Toxicol 2008; 21: 1841–1850. [PubMed: 18729331]

[43]. Hu X, Washington S, Verderame MF, Manni A. Interaction between polyamines and the mitogen-activated protein kinase pathway in the regulation of cell cycle variables in breast cancer cells. Cancer Res 2005; 65: 11026–11033. [PubMed: 16322252]

[44]. Koomoa DL, Yco LP, Borsics T, Wallick CJ, Bachmann AS. Ornithine decarboxylase inhibition by alpha-difluoromethylornithine activates opposing signaling pathways via phosphorylation of both Akt/protein kinase B and p27Kip1 in neuroblastoma. Cancer Res 2008; 68: 9825–9831. [PubMed: 19047162]

[45]. Jeter JM, Alberts DS. Difluoromethylornithine: the proof is in the polyamines. Cancer Prev Res (Phila) 2012; 5: 1341–1344. [PubMed: 23221207]

[46]. Glutathione Sies H. and its role in cellular functions. Free Radic Biol Med 1999; 27: 916–921. [PubMed: 10569624]

[47]. Valko M, Rhodes CJ, Moncol J, Izkovic M, Mazur M. Free radical metals and antioxidants in oxidative stress-induced cancer. Chem Biol Interact 2006; 160: 1–40. [PubMed: 16430879]

[48]. Li W, Yuan XM, Ivanova S, Tracey KJ, Eaton JW, Brunk UT. 3-Aminopropanal formed during cerebral ischaemia is a potent lysosomotropic neurotoxin. Biochem J 2003; 371: 429–436. [PubMed: 12513695]

[49]. Rabbani N, Thornalley PJ. Methylglyoxal, glyoxalase 1 and the dicarbonyl proteome. Amino Acids 2012; 42: 1133–1142. [PubMed: 20963454]

[50]. Kalapos MP. Where does plasma methylglyoxal originate from? Diabetes Res Clin Pract 2012; 99: 260–271. [PubMed: 23206674]

[51]. Lee JM, Johnson JA. An important role of Nrf2-ARE pathway in the cellular defense mechanism. J Biochem Mol Biol 2004; 37: 139–143. [PubMed: 15469687]

[52]. Osburn WO, Kensler TW. Nrf2 signaling: an adaptive response pathway for protection against environmental toxic insults. Mutat Res 2008; 659: 31–39. [PubMed: 18164232]

[53]. Dinkova-Kostova AT, Holtzclaw WD, Kensler TW. The role of Keap1 in cellular protective responses. Chem Res Toxicol 2005; 18: 1779–1791. [PubMed: 16359168]

[54]. Dinkova-Kostova AT, Talalay P. NAD(P)H: quinone acceptor oxidoreductase 1 (NQO1) a multifunctional antioxidant enzyme and exceptionally versatile cytoprotector. Arch Biochem Biophys 2010; 501: 116–123. [PubMed: 20361926]

[55]. Sasaki H, Sato H, Kuriyama-Matsumura K, Sato K, Maebara K, Wang H, et al. Electrophile response element-mediated induction of the cystine/glutamate exchange transporter gene expression. J Biol Chem 2002; 277: 44765–44771. [PubMed: 12235164]

[56]. Kwak MK, Kensler TW, Casero RA. Induction of phase 2 enzymes by serum oxidized polyamines through activation of Nrf2: effect of the polyamine metabolite acrolein. Biochem Biophys Res Commun 2003; 305: 662–670. [PubMed: 12763045]

[57]. Finkel T, Holbrook NJ. Oxidants oxidative stress and the biology of ageing. Nature 2000; 408: 239–247. [PubMed: 11089981]

[58]. Davis RJ. Signal transduction by the JNK group of MAP kinases. Cell 2000; 103: 239–252. [PubMed: 11057897]

[59]. Pietenpol JA, Stewart ZA. Cell cycle checkpoint signaling: cell cycle arrest versus apoptosis. Toxicology 2002; 181–182: 475–481.

[60]. Vermeulen K, Van Bockstaele DR, Berneman ZN. The cell cycle: a review of regulation deregulation and therapeutic targets in cancer. Cell Prolif 2003; 36: 131–149. [PubMed: 12814430]

[61]. Halliwell B, Gutteridge JMC. Free Radical Biology and Medicine, 3rd ed New York, US: Oxford University Press; 2007 pp. 220–236.

[62]. Onuki J, Chen Y, Teixeira PC, Schumacher RI, Medeiros MH, Van Houten B, Di Mascio P. Mitochondrial and nuclear DNA damage induced by 5-aminolevulinic acid Arch Biochem Biophys 2004; 432: 178–187. [PubMed: 15542056]

[63]. Huang Y, Pledgie A, Rubin E, Marton LJ, Woster PM, Sukumar S, et al. Role of p53/p21(Waf1/Cip1) in the regulation of polyamine analogue-induced growth inhibition and cell death in human breast cancer cells. Cancer Biol Ther 2005; 4: 1006–1013. [PubMed: 16131835]

[64]. Ueda A, Araie M, Kubota S. Polyamine depletion induces G1 and S phase arrest in human retinoblastoma Y79 cells. Cancer Cell Int 2008; 8: 2. [PubMed: 18208615]

[65]. Yamashita T, Nishimura K, Saiki R, Okudaira H, Tome M, Higashi K, et al. Role of polyamines at the G1/S boundary and G2/M phase of the cell cycle. Int J Biochem Cell Biol 2013; doi: 101016/jbiocel201302021.

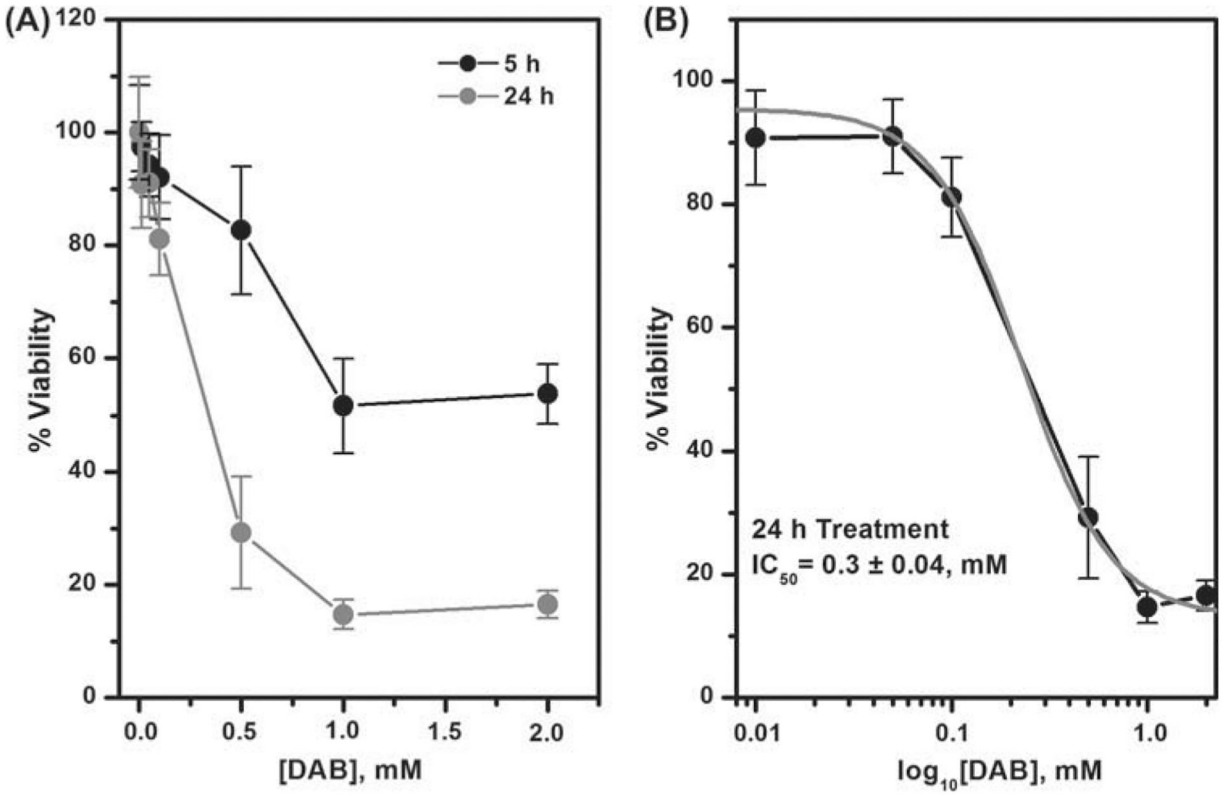

Figure 1. Viability of RKO cells exposed to DAB.

RKO cells are seeded in 96-well plates at a density of 8,000 cells/well in DMEM supplemented with 10% FBS 24 h prior to DAB treatment. All DAB assays are performed in phenol red-free OptiMEM-reduced serum medium. Cell viability is assessed by WST-1 reduction levels compared to controls. Cell viability at different DAB concentrations after 5 or 24 h of incubation (A). IC_{50} calculation from the cell viability of RKO cells after 24 h of treatment (B).

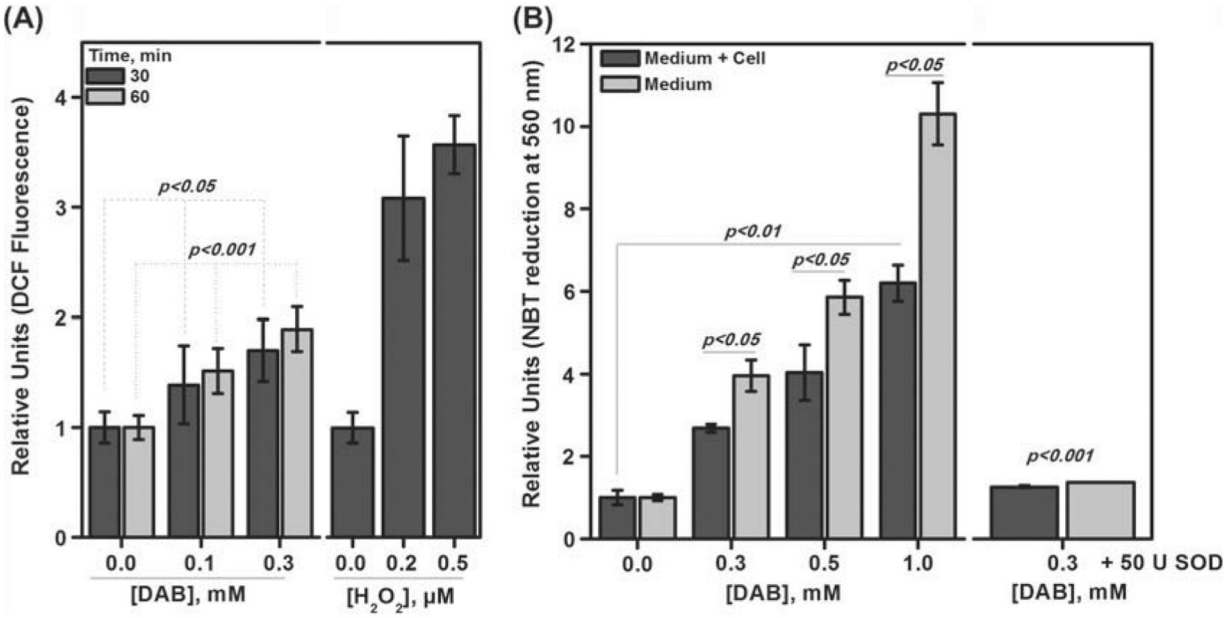

Figure 2. Effect of DAB on intra/extracellular redox status in RKO cells.

RKO cells are seeded in 96-well plates at 12,000 cells/well in DMEM supplemented with 10% FBS 24 h prior to each treatment. Cells are pre-loaded with fresh 30µM DCFH-DA in phenol red-free OptiMEM-reduced serum medium for 60 min at 37°C. The cells are subsequently rinsed thrice with PBS at RT and treated with different concentrations of DAB or H_2O_2. The fluorescence intensities are read at 488/530 nm immediately after the addition of DAB or H at the presented times (A). RKO cells are seeded in 24-well plate at 5×10^4 cells/well in DMEM supplemented with 10% FBS 24 h prior to the assay. The cells are incubated with different DAB concentrations in presence of 0.1% NBT prepared in phenol red free-MEM, supplemented with 2% FBS for 3 h at 37°C. The formazan product in the medium is measured at 560 nm. A control assay is performed with 0.3 mM DAB in presence of 50 U CuZnSOD (B).

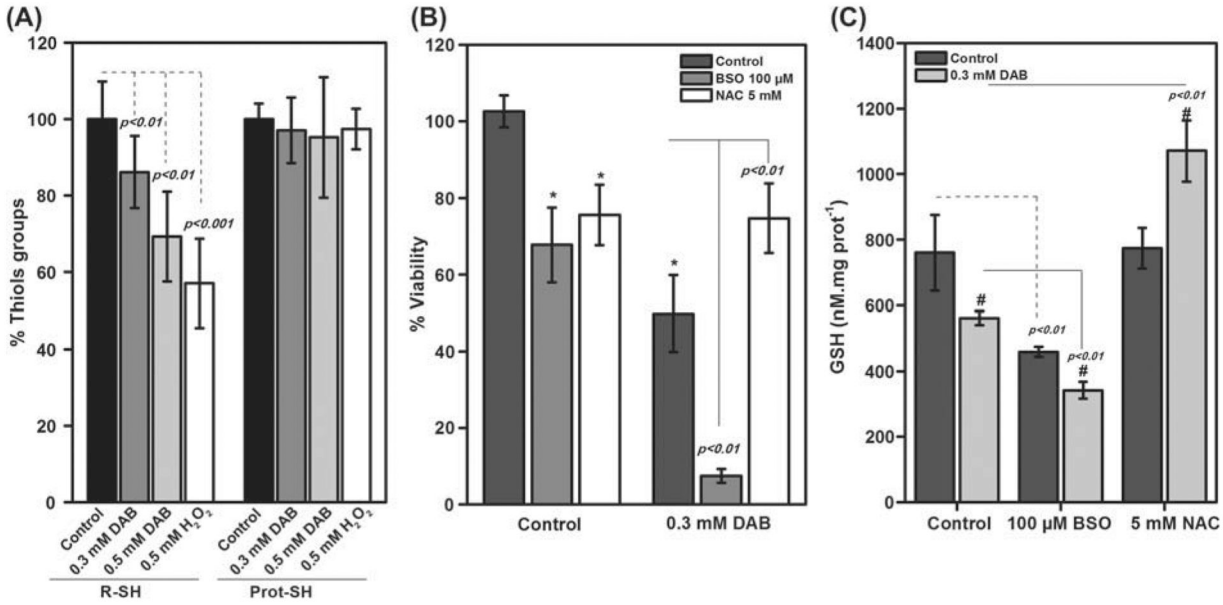

Figure 3. Levels of thiol groups and role of GSH in RKO cells under DAB treatment.

RKO cells (3.5×10^5) are treated with DAB or H_2O_2 for 5 h in OptiMEM. The total thiol groups are measured in TCA-precipitate, protein-SH and soluble fractions, and low molecular weight thiols. The thiol groups are accessed by reactions with monobromobimane (A). RKO cells (5×10^4) are pretreated with NAC or BSO in phenol red free-MEM, supplemented with 2% FBS for 24 h at 37°C. Subsequently, cells are treated with 0.3 mM DAB and after 24 h the viability was evaluated (B). RKO cells (3.5×10^5) are treated at the same conditions and the levels of GSH are measured by the enzymatic recycling method [23] (C).

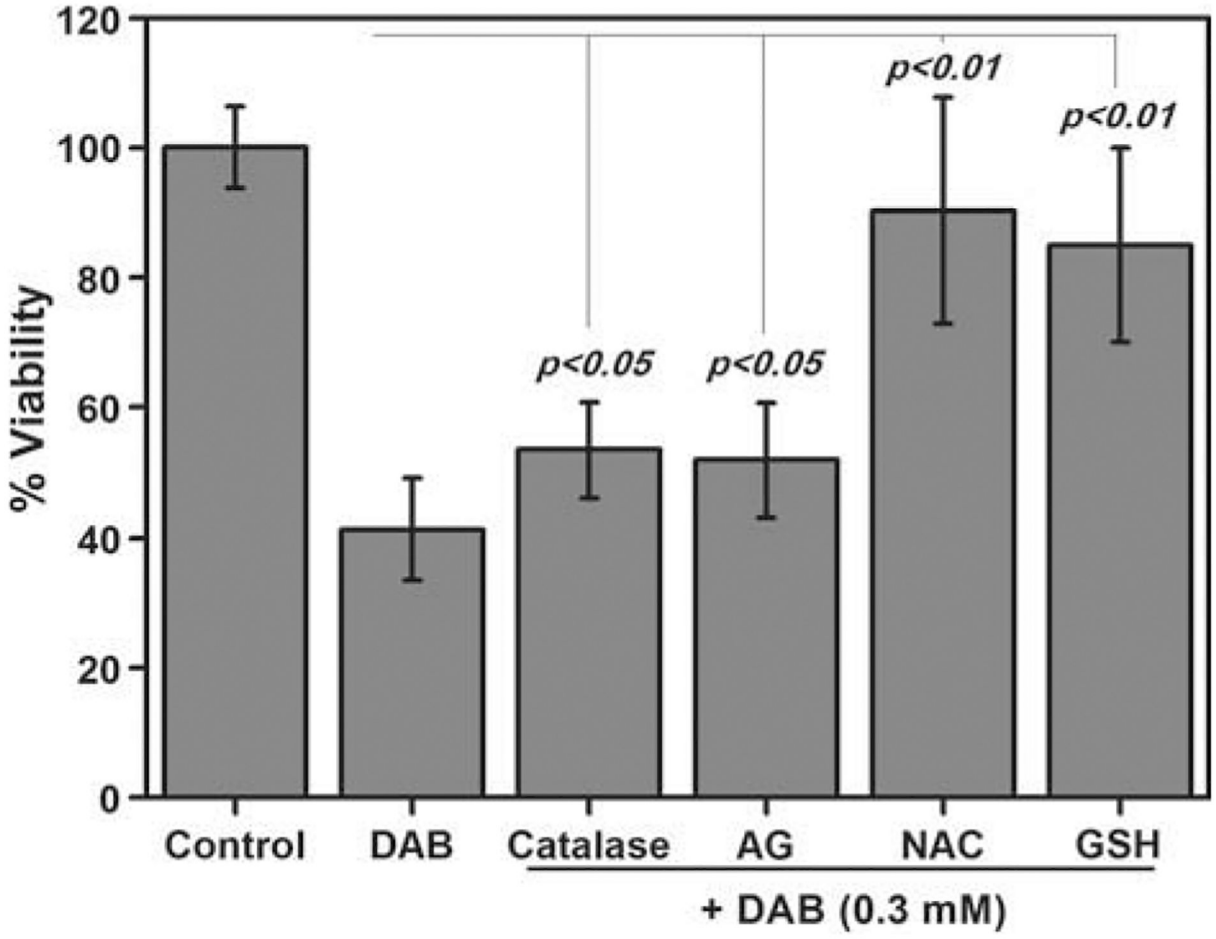

Figure 4. Effects of antioxidants on DAB toxicity to RKO cell line.

RKO cells are seeded in 24-well plates at 5×10^4 cells/well in DMEM supplemented with 10% FBS 24 h prior to treatments. The cells are treated with DAB in medium supplemented with 5 μM catalase, 20 mM aminoguanidine, 5 mM NAC or 5 mM GSH for 24 h in phenol red free-MEM, supplemented with 2% FBS.

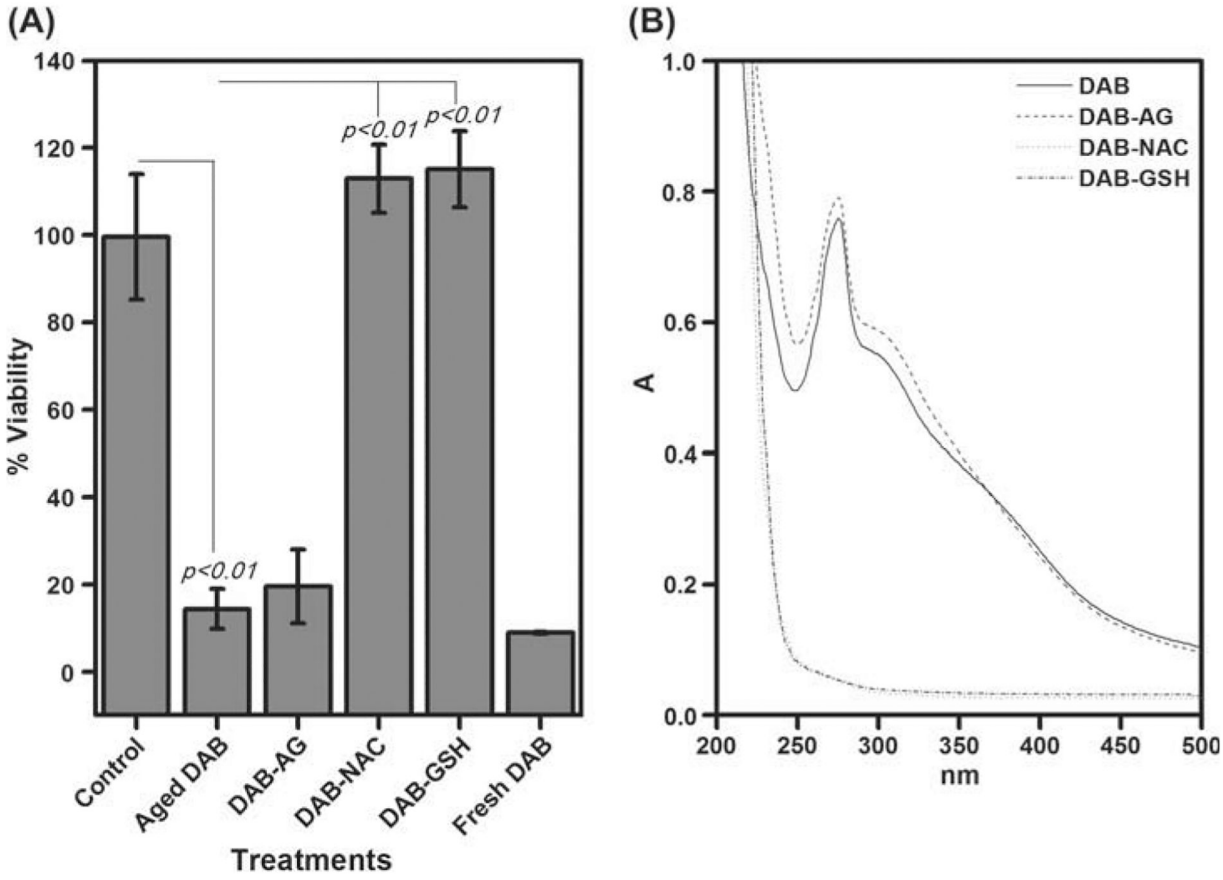

Figure 5. Effect of the cyclic end products of DAB oxidation (oxoDAB derivatives) on RKO viability.

RKO cells are seeded in 24-well plates at 5×10^4 cells/well in DMEM supplemented with 10% FBS 24 h prior to treatments. DAB (10 mM in PBS) is aged at 37°C for 24 h, in presence or absence of 20 mM of aminoguanidine, or NAC or GSH. The cells are treated with 1 mM of DAB-aged solution in phenol red free-MEM, supplemented with 2% FBS for 24 h (A). UV-Vis spectra of 24 h aged solutions of DAB in PBS in the presence and absence of 20 mM aminoguanidine, NAC or GSH. Spectra obtained from the DAB-NAC (dotted line) and DAB-GSH (dot-dashed line) systems are similar (B).

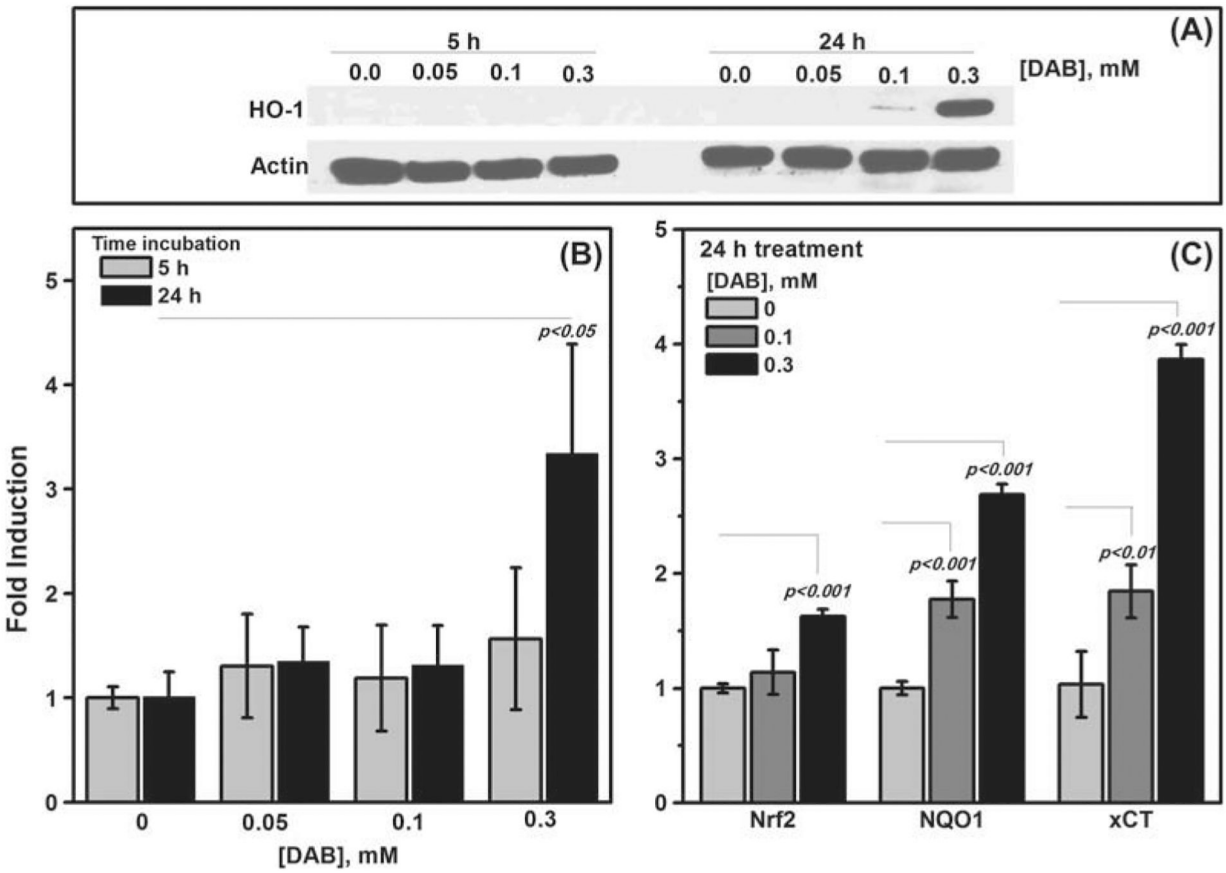

Figure 6. Effect of DAB on the expression of HO-1 and other antioxidant response factors.

RKO cells are seeded in 100 mm dish at a density of 2×10^6 cells in DMEM supplemented with 10% FBS 24 h prior to DAB treatment. RKO cells are treated with different concentrations of DAB during 5 or 24 h in phenol red-free OptiMEM-reduced serum medium. The cultures are maintained in a humidified atmosphere of 5% CO and 95% air at 37°C. Protein and RNA samples are submitted for to Western blot analysis (A) and RT-PCR analysis (B and C), respectively.

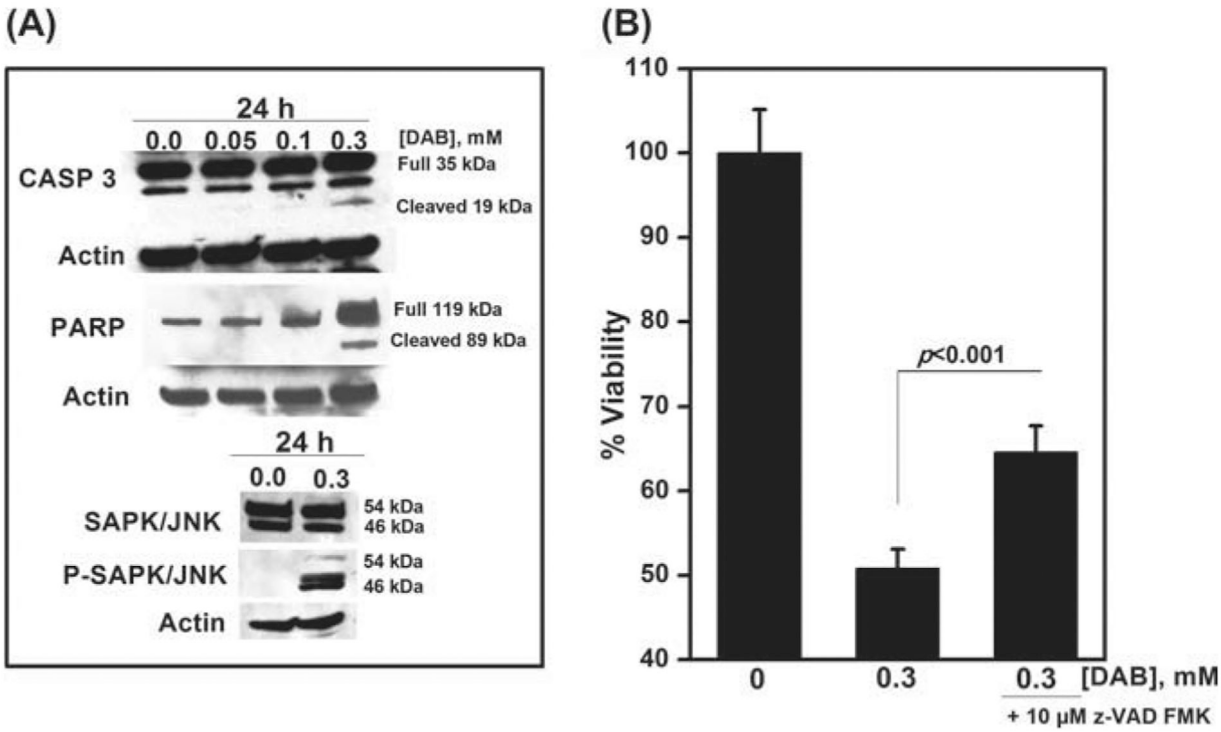

Figure 7. Effects of DAB on the apoptotic pathways of RKO cell lineage.

RKO cells are seeded in a 100 mm dish at a density of 2×10^6 cells in DMEM supplemented with 10% FBS 24 h prior to DAB treatment. RKO cells are treated with different concentrations of DAB for 24 h in phenol red-free OptiMEM-reduced serum medium. Protein samples are submitted to Western blot analysis using specific primary antibodies (A). The effect of pan-caspase inhibitors on DAB toxicity is evaluated by a cell viability assay using the WST-1 reagent, in which RKO cells are seeded at 8,000 cells/well in 96-well plates in DMEM supplemented with 10% FBS 24 h before each treatment. The cells are previously treated with 10 μM z-VAD-FMK, followed by DAB treatment for 24 h in phenol red-free OptiMEM-reduced serum medium (B).

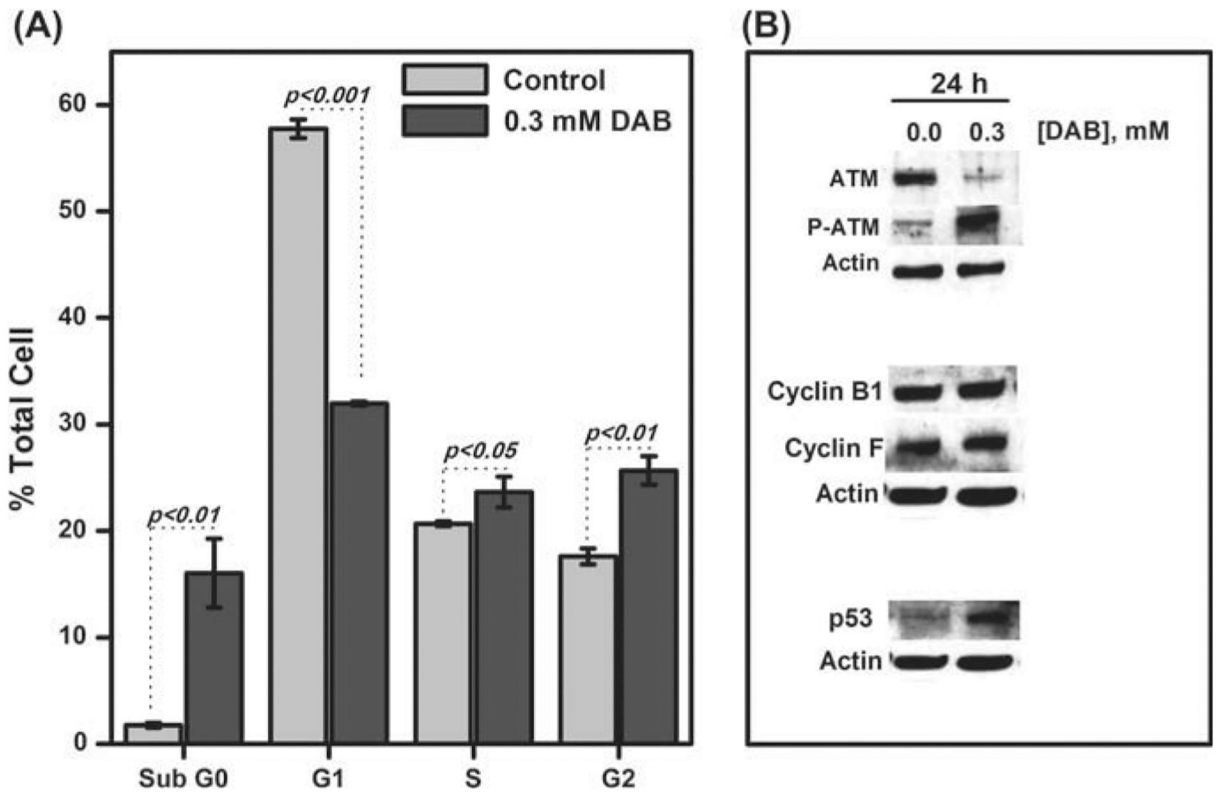

Figure 8. Effect of DAB treatment on cell cycle and related proteins.

RKO cells are treated with 0.30 mM DAB for 24 h in OptiMEM. After time-lapse incubation, the cell suspensions (2×10^6 cells/ml) are fixed in cold 70% ethanol overnight at 4°C, washed with PBS and stained with 50 μ g/mL iodide propidium solution in DPBS containing 50 μg/mL of RNase A for 30 min. The samples are analyzed by a flow cytometer (A). Protein samples are submitted to Western blotting analysis in which specific primary antibodies are used (B).

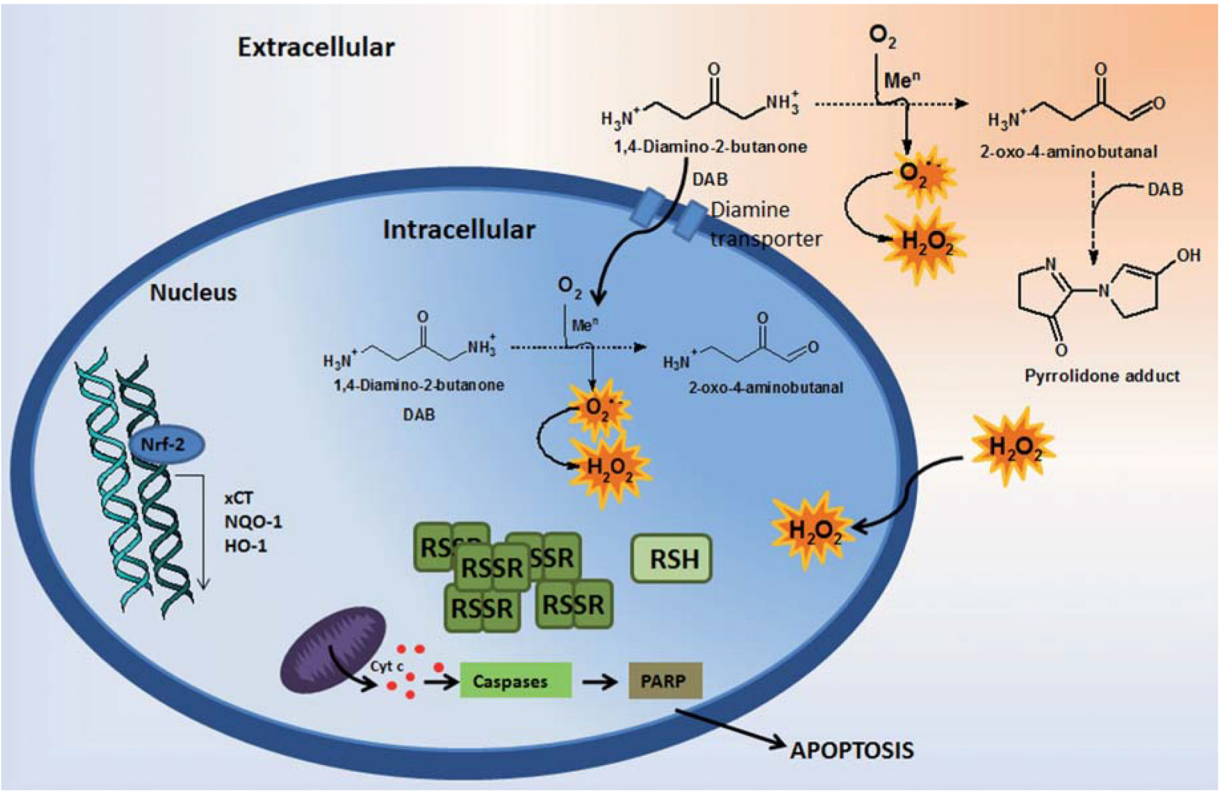

Figure 9. Envisaged mechanism to explain the cytotoxic effects of DAB on mammalian cells.

DAB undergoes metal-catalyzed aerobic oxidation yielding oxyradicals and an α-oxoaldehyde at both extra and intracellular environments. Increased ROS levels changes the cell redox balance leading to depletion of protective thiols. The resulting oxidizing triggers up-regulated stress response pathways such as Nrf-2, HO-1, NQO1 and xCT, as well as leading to activation of caspases cascades, PARP cleavage and subsequently apoptosis.